Stress Fields Near Crack Tip in Elastic–Perfectly Plastic Crystals

TZU-CHIANG WANG

Institute of Mechanics, Academia Sinica, Beijing, PRC

1. Introduction

In recent years crack tip stress and deformation fields for elastic-plastic crystals have attracted scientist's attention.

Rice and Nikolic [1] have firstly presented the analysis of elastic perfectly plastic crack tip response of crystals in anti-plane shear. The nearest work given by Rice [3] shows the crack tip stress and deformation fields for tensile loaded perfectly plastic crystals. The crack tip fields are assembled by four angular sectors and shown to change discontinuously from sector to sector for stationary crack. The asymptotic solution of growing crack consists of also four angular sectors.

But as pointed out by Rice [3], the asymptotic solution is not unique. This paper presents the analysis of crack tip stress and deformation fields for tensile loaded elastic-perfectly plastic crystals.

The basic equations of plane strain problem for the elastic-perfectly plastic crystals with double slip systems have been presented in the basis of three-dimensional flow theory of crystal plasticity. Using these equations, the stationary crack tip fields are analysed for tensile load.

The fields are assembled by three angular sectors. The stress and displacement fields are fully continuous.

The assembly of growing crack tip field involves five angular sectors. The present solutions contain a free parameter and give a family of crack tip fields.

Finally the application of these solutions of the FCC and BCC crystals are considered.

2. Basic Equation

For the sake of simplicity, we start from the analysis of double slip plane model of crystal proposed by Asaro [4].

As shown in Fig. 1, the plane model of double slip involves two slip systems: the primary slip system and the conjugate slip system.

(1). Yield Condition

According to the Schmid rule, the yield condition for elastic-perfectly plastic crystals can be expressed

$$\tau^{(\alpha)} = \tau_c^{(\alpha)} = \tau_c \ , \tag{2.1}$$

where $\tau^{(\alpha)}$ is the resolved shear stress of the αth slip system, $\tau_c^{(\alpha)}$ is the critical shear stress of the αth slip system.

In the polar coordinates (r,θ), we have

$$\left.\begin{aligned} \tau^{(1)} &= -\frac{1}{2}(\sigma_\theta - \sigma_r)\sin 2(\theta-\phi_o) + \tau_{r\theta}\cos 2(\theta-\phi_o) \ , \\ \tau^{(2)} &= \frac{1}{2}(\sigma_\theta - \sigma_r)\sin 2(\theta+\phi_o) - \tau_{r\theta}\cos 2(\theta+\phi_o) \ . \end{aligned}\right\} \tag{2.2}$$

(2). Constitutive Relation

The constitutive relation of crystals can be taken in the form,

$$D_{ij} = \frac{(1+\nu)}{E}\dot{\sigma}_{ij} - \frac{\nu}{E}\delta_{ij}\dot{\sigma}_{kk} + D^p_{ij} \ , \tag{2.3}$$

where D_{ij} is the strain rate tensor. D^p_{ij} is the plastic strain rate tensor,

$$\underset{\sim}{D}^p = \sum_{\alpha=1}^{n} \underset{\sim}{P}^{(\alpha)} \dot{\gamma}^{(\alpha)}, \quad n = 4 \ , \tag{2.4}$$

here $\dot{\gamma}^{(\alpha)}$ is the slip shear rate of the αth slip system.

3. Stress and Deformation Fields Near a Stationary Crack

As shown in Fig. 2, the crack tip zone is assembled by three angular sectors. The domains A and C are plastic zones and the domain B is an elastic zone.

Consider a pure mode I crack. Due to symmetry, we only consinder the upper half plane.

In domain A, two slip systems will simultaneously attain yield. From the first equation of formula (2.1), we obtain

$$F = \frac{\tau_c}{2\sin 2\phi_o}[\cos 2\theta + \bar{A}_1] \ , \tag{3.1}$$

Similarly we obtain (in domain c),

$$F = \frac{k^*}{2}[1-\cos 2\theta] \ , \quad k^* = \frac{\tau_c}{\sin 2\phi_o} \ , \tag{3.2}$$

In elastic zone B, we have

$$F = \frac{k^*}{2}[1-\cos 2\theta] + B_1^*[\theta - \bar{\beta} - \frac{1}{2}\sin 2(\theta+\beta)] \ , \tag{3.3}$$

here $\bar{\beta} = \pi - \beta$, β is the angle between the boundary Γ_B and the crack face.

From the complete continuity of stress components on boundary Γ_A, we find

$$\left.\begin{aligned} \frac{k^*}{2}(\bar{A}_1 + \cos 2\alpha) &= \frac{k^*}{2}(1-\cos 2\alpha) + B_1^*[\alpha+\beta-\pi-\frac{1}{2}\sin 2(\alpha+\beta)] \ , \\ -k^*\sin 2\alpha &= k^*\sin 2\alpha + B_1^*[1-\cos 2(\alpha+\beta)] \ , \\ -2k^*\cos 2\alpha &= 2k^*\cos 2\alpha + 2B_1^*\sin 2(\alpha+\beta) \ . \end{aligned}\right\} \tag{3.4}$$

We have

$$\left.\begin{aligned} \alpha &= \beta \ , \quad B_1^* = -k^*/\sin 2\alpha \ , \\ \bar{A}_1 &= 1 + 2(\pi-2\alpha)/\sin 2\alpha \ , \end{aligned}\right\} \tag{3.5}$$

Since the yield constraint condition should be satisfied in domain B, hence we have $\alpha = \beta \geqslant \phi_o$, $\alpha = \beta \geqslant \pi/2 - \phi_o$.

4. Stress and Deformation Fields Near a Growing Crack Tip

The possible option is shown in Fig. 3. The assembly of sectors involves five angular sectors. The domains A and B are constant stress zones; domains C and D are elastic unloading zones; domain E is a secondary plastic zone. The velocity discontinuity may occur on boundary Γ_A, Γ_B, and Γ_C. As pointed out by Rice [3], the velocity discontinuity ray must have the direction of slip plane traces or normal traces of slip plane. Hence we have

$$\alpha = \mathrm{Min}\,(\phi_o \ , \ \frac{\pi}{2} - \phi_o) \ ,$$

$$\beta = \mathrm{Max}\,(\phi_o \ , \ \frac{\pi}{2} - \phi_o) \ ,$$

When $\phi_o \geqslant \frac{\pi}{4}$, we have

$$\alpha = \frac{\pi}{2} - \phi_o \ , \quad \beta = \phi_o \ .$$

Thus the velocity jump is slip-type shear on Γ_B but kinking-type shear on Γ_A.

The stress function of an asymptotic field can be expressed as

$$\phi = r^2 F(\theta) \ , \tag{4.1}$$

$$F(\theta) = \begin{cases} \dfrac{k^*}{2}[\bar{A}_1 + \cos 2\theta] \ , & \text{in domains A and B} \\[2ex] \dfrac{C_1^*}{4} F_s(\theta) + \dfrac{C_2^*}{4}\theta + C_3 + C_4[1-\cos(\theta-\beta)] + C_5 \sin 2(\theta-\beta) \ , & \text{in domain C} \\[2ex] \dfrac{D_1^*}{4} F_s(\theta) + \dfrac{D_2^*}{4}\theta + D_3 + D_4[1-\cos 2(\theta-\bar{\gamma})] + D_5 \sin 2(\theta-\bar{\gamma}) \ , & \text{in domain D} \\[2ex] \dfrac{k^*}{2}[1-\cos 2\theta] \ , & \text{in domain E} \end{cases} \tag{4.2}$$

and

$$F_s(\theta) = (1-\cos 2\theta)\,\mathrm{Ln}\sin\theta - \theta \cdot \sin 2\theta - \cos^2\theta \ , \tag{4.3}$$

Due to continuity of stress components on Γ_B, we find

$$\left.\begin{aligned} C_3 &= \frac{k^*}{2}(\bar{A}_1 + \cos 2\beta) - \frac{C_1^*}{4} F_s(\beta) - \frac{C_2^*}{4}\beta \ , \\ C_4 &= -\frac{k^*}{2}\cos 2\beta - \frac{C_1^*}{4}(\mathrm{Ln}\sin\beta - F_s(\beta)) \ , \\ C_5 &= -\frac{k^*}{2}\sin 2\beta - \frac{C_1^*}{4}\cdot\frac{F_s'(\beta)}{2} - \frac{C_2^*}{8} \ . \end{aligned}\right\} \tag{4.4}$$

The continuity of stress components on Γ_D results in

$$\left.\begin{aligned} D_3 &= \frac{k^*}{2}(1-\cos 2\bar{\gamma}) - \frac{D_1^*}{4} F_s(\bar{\gamma}) - \frac{D_2^*}{4}\bar{\gamma} \ , \\ D_4 &= \frac{k^*}{2}\cos(2\bar{\gamma}) - \frac{D_1^*}{4}[\mathrm{Ln}\sin\bar{\gamma} - F_s(\bar{\gamma})] \ , \\ D_5 &= \frac{k^*}{2}\sin 2\bar{\gamma} - \frac{D_1^*}{4}\cdot\frac{F_s'(\bar{\gamma})}{2} - \frac{1}{8}D_2^* \ . \end{aligned}\right\} \tag{4.5}$$

From the stress continuity of Γ_C, it follows

$$\frac{(C_1^*-D_1^*)}{4} F_s(\bar{\beta}) + \frac{(C_2^*-D_2^*)}{4}\bar{\beta} + (C_3-D_3) + C_4[1-\cos 2(\bar{\beta}-\beta)] + C_5 \sin 2(\bar{\beta}-\beta)$$
$$- D_4[1-\cos 2(\bar{\beta}-\bar{\gamma})] - D_5 \sin 2(\bar{\beta}-\bar{\gamma}) = 0 \ , \tag{4.6}$$

$$\frac{1}{4}(C_1^*-D_1^*) F_s'(\bar{\beta}) + \frac{1}{4}(C_2^*-D_2^*) + 2C_4 \sin 2(\bar{\beta}-\beta) + 2C_5 \cos 2(\bar{\beta}-\beta)$$
$$- 2D_4 \sin 2(\bar{\beta}-\gamma) - 2D_5 \cos 2(\bar{\beta}-\gamma) = 0 \ , \tag{4.7}$$

$$(C_1^*-D_1^*)(\mathrm{Ln}\sin\bar{\beta} - F_s(\bar{\beta})) + 4C_4 \cos 2(\bar{\beta}-\beta) - 4C_5 \sin 2(\bar{\beta}-\beta)$$
$$- 4D_4 \cos 2(\bar{\beta}-\bar{\gamma}) - 4D_5 \sin 2(\bar{\beta}-\bar{\gamma}) = 0 \ , \tag{4.8}$$

On Γ_C, velocity jump occurs, we have

$$\tau^{(2)} = -\tau_c \ , \quad (\text{or } \tau^{(1)} = -\tau_c) \tag{4.9}$$

On the other hand, the normal velocity component must be continuously across the Γ_C, it yields

$$C_1^* \sin\bar{\beta} - C_2^* \cos\bar{\beta} = D_1^* \sin\bar{\beta} - D_2^* \cos\bar{\beta} \ , \tag{4.10}$$

The calculation is carried out for $\phi_o = 54.74°$.

The calculation shows that the correct solution is obtained for each γ when $9.009° \le \gamma \le 12.7°$. The solutions satisfy all asymptotic equations and full constraint conditions.

Fig. 4 shows the stress distribution along a circumferential direction for $\gamma = 9.009°$.

5. Application on FCC and BCC Crystals

The crystal axis coordinates for FCC and BCC crystals have been shown in Fig. 5. The X_c, Y_c, and Z_c axes are along the [100], [010], and [001] directions respectively. The fixed Cartesian coordinates 0XYZ used in the previous sections are also shown in Fig. 5.

The equal slip along the $[1\bar{1}0]$ and $[01\bar{1}]$ directions on the slip plane (111) will result in slip along $[1\bar{2}1]$, and yield plane strain deformation. We have,

$$\begin{aligned} \underset{\sim}{D}^P &= (\underset{\sim}{P}_A^{(2)} + \underset{\sim}{P}_B^{(2)})\,\dot{\gamma}^{(2)} \\ &= \frac{1}{2}\left\{(\underset{\sim}{m}_A^{(2)} + \underset{\sim}{m}_B^{(2)}) \otimes \underset{\sim}{n}^{(2)} + \underset{\sim}{n}^{(2)} \otimes (\underset{\sim}{m}_A^{(2)} + \underset{\sim}{m}_B^{(2)})\right\}\dot{\gamma}^{(2)} \\ &= \frac{\sqrt{3}}{2}\left\{\underset{\sim}{m}^{(2)} \otimes \underset{\sim}{n}^{(2)} + \underset{\sim}{n}^{(2)} \otimes \underset{\sim}{m}^{(2)}\right\}\dot{\gamma}^{(2)} = \sqrt{3}\,\underset{\sim}{P}^{(2)}\,\dot{\gamma}^{(2)} \ , \end{aligned} \tag{5.1}$$

where

$$\left.\begin{aligned} \underset{\sim}{P}^{(2)} &= \frac{1}{2}(\underset{\sim}{m}^{(2)} \otimes \underset{\sim}{n}^{(2)} + \underset{\sim}{n}^{(2)} \otimes \underset{\sim}{m}^{(2)}) , \\ \underset{\sim}{m}_A^{(2)} + \underset{\sim}{m}_B^{(2)} &= \sqrt{3}\, \underset{\sim}{m}^{(2)} . \end{aligned}\right\} \tag{5.2}$$

Similarly for slip systems $(\bar{1}1\bar{1})$ [011] and $(\bar{1}1\bar{1})$ [110], we have

$$\underset{\sim}{D}^{P} = \sqrt{3}\, \underset{\sim}{P}^{(1)} \dot{\gamma}^{(1)} , \tag{5.3}$$

here

$$\underset{\sim}{P}^{(1)} = \frac{1}{2}(\underset{\sim}{m}^{(1)} \otimes \underset{\sim}{n}^{(1)} + \underset{\sim}{n}^{(1)} \otimes \underset{\sim}{m}^{(1)}) , \tag{5.4}$$

From Eqs. (5.1) and (5.3), we find

$$\underset{\sim}{D}^{P} = \sqrt{3}\, (\underset{\sim}{P}^{(1)} \dot{\gamma}^{(1)} + \underset{\sim}{P}^{(2)} \dot{\gamma}^{(2)}) \tag{5.5}$$

In comparing Eq. (5.4) with Eq. (2.4), it can be found that the problem of FCC crystals discussed here is equivalent to the corresponding problem of double slip crystals, if we take $\sqrt{3}\dot{\gamma}^{(1)}$ and $\sqrt{3}\dot{\gamma}^{(2)}$ considered here to be equal to $\dot{\gamma}^{(1)}$ and $\dot{\gamma}^{(2)}$ of that considered on double slip crystals.

Therefore the above results can be immediately applied on plane strain crack problems of the FCC and BCC crystals.

References

[1] Rice, J.R. and Nikolic, R., J. Mech. Phys. Solids, 33 (1985), 595-622.

[2] Rice, J.R. and Saeedvafa, M., J. Mech. Phys. Solids, 34 (1987), in press.

[3] Rice, J.R., Mechanics of Materials, 1987, in press.

[4] Asaro, R.J., J. Appl. Mech., 50 (1983), 921-934.

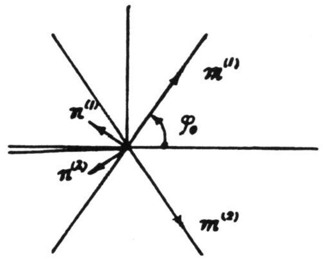

Fig. 1 Double slip plane model of a crystal.

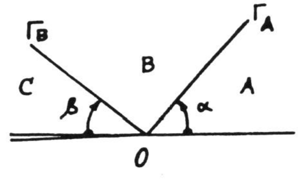

Fig. 2 Assembly of angular sectors for a stationary crack.

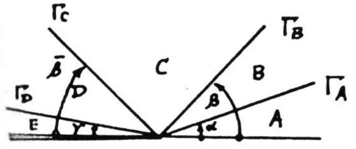

Fig. 3 Assembly of angular sectors near the growing crack tip.

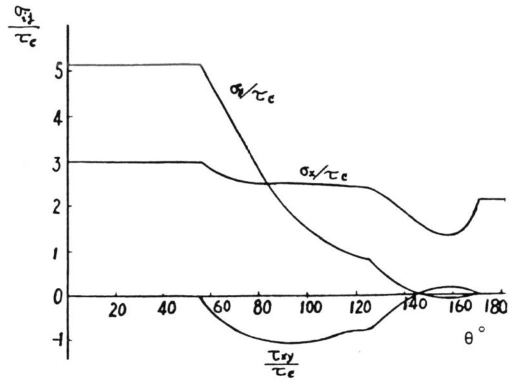

Fig. 4 Stress distribution along the circumferential direction for γ = 9.009°.

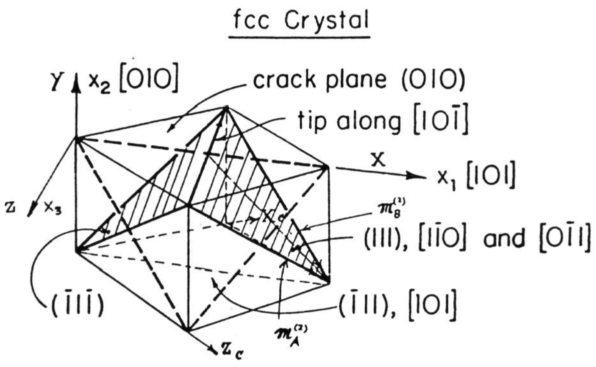

Fig. 5 FCC crystal and coordinate systems.